REPORT DOCUMENTATION PAGE

Form Approved
OMB No. 074-0188

1. AGENCY USE ONLY (Leave blank)	2. REPORT DATE	3. REPORT TYPE AND DATES COVERED
	Oct. 1-Dec. 31, 1995	Quarterly report, October 1- December 31, 1995

4. TITLE AND SUBTITLE
Kinetics of Supercritical Water Oxidation

5. FUNDING NUMBERS
N/A

6. AUTHOR(S)
Steven F. Rice

7. PERFORMING ORGANIZATION NAME(S) AND ADDRESS(ES)
Sandia National Laboratories
Combustion Research Facility

MIT

Princeton University

8. PERFORMING ORGANIZATION REPORT NUMBER
Case 8610.000

9. SPONSORING / MONITORING AGENCY NAME(S) AND ADDRESS(ES)
SERDP
901 North Stuart St. Suite 303
Arlington, VA 22203

10. SPONSORING / MONITORING AGENCY REPORT NUMBER
N/A

11. SUPPLEMENTARY NOTES
Prepared for Sandia National Laboratories, Combustion Research Facility, Case 8610.000. This work was supported in part by SERDP.

12a. DISTRIBUTION / AVAILABILITY STATEMENT
Approved for public release: distribution is unlimited

12b. DISTRIBUTION CODE
A

13. ABSTRACT ***(Maximum 200 Words)***

This project consists of experiments and theoretical modeling designed to improve our understanding of the detailed chemical kinetics of supercritical water oxidation (SCWO) processes. The objective of the three year project is to develop working models that accurately predict the oxidation rates and mechanisms for a variety of key organic species over the range of temperatures and pressures important for industrial applications. Our examination of reaction kinetics in supercritical water undertakes *in situ* measurements of reactants, intermediates, and products using optical spectroscopic techniques, primarily Raman spectroscopy. Our focus is to measure the primary oxidation steps that occur in the oxidation of methanol, higher alcohols, methylene chloride, and some simple organic compounds containing nitro groups. We are placing special emphasis on identifying reaction steps that involve hydroxyl radical, hydroperoxyl radical, and hydrogen peroxide. The measurements are conducted in two optically accessible reactors, the supercritical flow reactor (SFR) and the supercritical cell reactor (SCR), designed to operate at temperatures and pressures up to 600^{0}C and 500 MPa. The combination of these two reactors permit reaction rate measurements raging from 0.1 s to many hours.

14. SUBJECT TERMS
supercritical water oxidation (SCWO), optical spectroscopic techniques, Raman spectroscopy, SERDP

15. NUMBER OF PAGES
28

16. PRICE CODE
N/A

17. SECURITY CLASSIFICATION OF REPORT	18. SECURITY CLASSIFICATION OF THIS PAGE	19. SECURITY CLASSIFICATION OF ABSTRACT	20. LIMITATION OF ABSTRACT
unclass	unclass	unclass	UL

Kinetics of Supercritical Water Oxidation
SERDP Compliance Technical Thrust Area

Quarterly Report

Sandia National Laboratories
Combustion Research Facility
Case 8610.000

Principal Investigator:	Steven F. Rice, Sandia
Project Associates, Sandia:	Richard R. Steeper, Thomas B. Hunter, Russell G. Hanush, Jason D. Aiken,
University Collaborators:	Jefferson W. Tester, MIT Kenneth Brezinsky, Princeton University
Project Manager:	Donald R. Hardesty
Reporting Period:	October 1 - December 31, 1995

Project description

This project consists of experiments and theoretical modeling designed to improve our understanding of the detailed chemical kinetics of supercritical water oxidation (SCWO) processes. The objective of the three-year project is to develop working models that accurately predict the oxidation rates and mechanisms for a variety of key organic species over the range of temperatures and pressures important for industrial applications. Our examination of reaction kinetics in supercritical water undertakes *in situ* measurements of reactants, intermediates, and products using optical spectroscopic techniques, primarily Raman spectroscopy. Our focus is to measure the primary oxidation steps that occur in the oxidation of methanol, higher alcohols, methylene chloride, and some simple organic compounds containing nitro groups. We are placing special emphasis on identifying reaction steps that involve hydroxyl radicals, hydroperoxyl radicals, and hydrogen peroxide. The measurements are conducted in two optically accessible reactors, the supercritical flow reactor (SFR) and the supercritical cell reactor (SCR), designed to operate at temperatures and pressures up to 600°C and 500 MPa. The combination of these two reactors permit reaction rate measurements ranging from 0.1 s to many hours.

The work conducted here continues the experimental approach from our previous SERDP-funded project by extending measurements on key oxidant species and

expanding the variety of experimental methods, primarily optical in nature, that can be used to examine reactions at SCWO conditions. Direct support is provided to the project collaborators at MIT and Princeton who are contributing to model development for phenol and halogenated species. These researchers are examining these processes using more conventional sample-and-quench methods. The experiments at Sandia and at the universities all focus on determining the primary oxidation steps that involve the OH and HO_2 radicals, generating data that will be used to evaluate and refine SCWO reaction kinetic schemes. The primary technical difficulty in this stage of the project will be recasting existing high temperature (1100 °C) chemical kinetic models for these simple molecules to 400-600 °C. At these temperatures, the role of the HO_2 radical becomes important.

Executive Summary of Progress this Period

Programmatic

The most important programmatic event this quarter was the departure of Tom Hunter, the team's postdoctoral associate, to permanent employment at 3M Company in Minnesota. Tom was a key asset to the productivity of the team over the past 15 months whose skills and commitment to the project will be greatly missed. We are actively seeking a replacement for him. Fortunately, Dr. Eric Croiset arrives from CNRS Orleans in France during the first week of the next quarter. He will be visiting us for one year and working entirely on this project. We are in the process of arranging for the participation in the project of two summer students from Princeton University and Brown University for the June - August, 1996 period.

During this quarter, a meeting was held at Princeton University involving S.F. Rice, K. Brezinsky, I. Glassman, M. Pecullan to review progress and coordinate efforts on the phenol/anisole model development. We are arranging for Melissa Pecullan, a graduate student who is working on the phenol/anisole experiments at Princeton University with Dr. Brezinsky, to join us at Sandia for the summer. Also this quarter, S.F. Rice attended an Army Research Office Workshop at MIT. This workshop will produce a focused report exploring the application of SCWO to the cleanup of non-stockpile chemical warfare agents and the research needed to be done to realize this goal.

We have begun to participate on a project (supported by ARPA with Sandia's Engineering for Transportation and Environment Department) that is designed to develop SCWO technology for application to treat Navy shipboard excess hazardous material (EHM). The project is being conducted in close collaboration with Foster Wheeler Development Corp. and Aerojet Corp.

Finally this quarter, two milestone reports for the project were issued. R.R. Steeper completed his Ph.D. thesis last quarter and his thesis has been issued as a detailed

project milestone and Sandia Technical Report. A much-needed report describing in detail the operation of the Supercritical Fluids Reactor (SFR) was also issued as a Sandia Technical Report. These reports were broadly distributed to the SCWO community and additional copies may be obtained by contacting S.F. Rice.

Methane and methanol oxidation

Work this quarter continued to focus on interpreting the C_1 oxidation model that performed well for methanol and attempting to relate it to methane oxidation experimental results and other models. The main effort was devoted toward comparing the results from the Gas Research Institute's (GRI) high temperature gas phase methane oxidation model to our experimental results. The investigation showed excellent agreement between the model predictions and experiment; much better than we had anticipated. We have chosen to used this mechanism as a starting point for a SCWO model that connects methanol and methane oxidation at SCWO conditions to higher temperature chemistry and to use this as a base for describing larger molecule reactivity. After two papers are written, we will have completed our work in methane and methanol for the purposes of this project.

Propanol oxidation

Most of the experimental work this quarter was directed at completing the data set for isopropanol and n-propanol oxidation. These experiments were completed and showed some surprising results. We had expected n-propanol to be more stable than isopropanol, but the experiments revealed the opposite. We have characterized the loss of fuel as well as the production of CO and CO_2 in these similar systems. A paper is in preparation.

CO/CO_2 water-gas shift chemistry

Experimental work continued on the reaction of CO in water to form CO_2 and H_2. This system was chosen as an example of a simple reaction that can be characterized in terms of the role water can play in affecting the rate of reaction in this high-pressure, high-temperature environment. In contrast to the situation at low pressure, under SCWO conditions, our analysis this quarter reveals that that CO_2 continues to react at a slow rate to form another species, perhaps H_2CO_3. As a result, characterizing the overall reaction of $CO+H_2O$ => [H_2CO_2 (formic acid)] => CO_2+H_2 is complicated by CO_2+H_2O => H_2CO_3, disturbing the CO/CO_2 equilibrium. Another possibility is that there is an additional side reaction of CO with water at these conditions, forming carbon-containing species other than CO_2.

Princeton University, Mechanical and Aerospace Engineering Dept.

This quarter, species mole-fraction-versus-time profiles for intermediates formed during the high-temperature, low-pressure pyrolysis and oxidation of anisole (C_6H_5-O-CH_3) were obtained and preparation for the ensuing water addition experiments was completed. A parallel modeling effort was undertaken using, as a starting point, an existing 130 step reaction mechanism developed for the oxidation of benzene and toluene. However, much of the phenoxy-methyl recombination chemistry present in the anisole system, especially in the presence of water, is unknown and must be estimated to extend the existing simple hydrocarbon model.

Massachusetts Institute of Technology, Dept. of Chemical Engineering

During this quarter, important upgrades to the supercritical water flow reactor at MIT were completed. The method of using hydrogen peroxide as a source of high pressure oxygen in supercritical water has been incorporated into the system allowing a much wider range of feed concentration to be accessed. Detailed measurements have been conducted to confirm that the H_2O_2 is fully converted to O_2 before injection into the reactor. Concerns over the effectiveness of the mixing of the reactant flows has prompted an investigation into different configurations for optimizing this process. A new design using a side-entry inlet tee was fabricated and installed. Characterization of the performance of this improvement in design using methanol oxidation will hopefully lead to a reconciliation of some discrepancies between the experimental results obtained at Sandia and MIT over the past several years. In addition, the literature research required to arrive at this optimal design will be used to improve the performance of the Supercritical Fluids Reactor (SFR) at Sandia, flow reactors in other laboratories, and ultimately in commercial reactor designs.

Future work

During this quarter, our experimental work on the SERDP project will be directed at initiating high pressure experiments on phenol. The phenol work is now possible with the modifications made in 9/95 to the SFR that successfully eliminates pyrolysis reactions in the preheater. Our experimental work conducted 3/95 had shown that at temperatures above 500 °C pyrolysis of phenol was occurring in supercritical water solution in the preheater. Experiments will continue collecting data on the water gas shift reaction at higher pressure and identifying the nature of the side product that appears to be formed. Finally, we intend to complete and submit the manuscripts for three papers on the following topics: propanol oxidation, application of the GRI model to supercritical water conditions, and optical cell design. In addition, considerable time will be devoted to the ARPA project mentioned above in the Programmatic section. This work is in direct response to a Navy need to find a solution for disposal of shipboard excess hazardous material.

At Sandia, our participation in the SERDP project provides considerable leveraging of research equipment and personnel for this application of SCWO to DoD environmental regulation compliance.

Publications & presentations

R. G. Hanush, S. F. Rice, T. B. Hunter, and J. D. Aiken, "Operation and Performance of the Supercritical Fluids Reactor (SFR)" (Sandia National Laboratories Report SAND-8203, Livermore, CA, 1995).

R. R. Steeper, "Methane and Methanol Oxidation in Supercritical Water: Chemical Kinetics and Hydrothermal Flame Studies" (Sandia National Laboratories Report SAND-8208, Livermore, CA, 1995).

Detailed Summary of Technical Progress this Period

Methane and methanol oxidation modeling

The goal of this activity is to make a connection between the high-pressure, low-temperature predictions from recent experiments in supercritical water to the "best effort" at representing oxidation of C_1 species at combustion conditions. It is important to establish this relationship with the smallest amount of customization as possible, with all of the parameters for both the mechanism and thermodynamics originating from a single, well-documented source and the computation conducted in a well-established code. We have applied the recently developed GRI 1.2 mechanism[1] to the oxidation of methane and methanol at 250 bar and 420 - 630 °C. The results from the mechanism applied in the Chemkin II computational package have been compared with a variety of experiments on these two fuels. These calculations show that the GRI 1.2 mechanism reproduces almost all experimental results on methane very accurately. In addition, good agreement for fuel consumption and formaldehyde production during methanol oxidation can be obtained with the inclusion of two critical reactions and the modification of the parameters for a third involving HO_2. There are several important observations regarding the reactivity of HO_2 and CH_3O_2 in these systems leading to implications for the extension of the GRI mechanism to lower temperatures when contrasted with two other recently proposed mechanisms. We have observed that, to compare different experimental results from different sources, the experimental concentration range must be considered.

Methods

The GRI 1.2 mechanism is accompanied by a Chemkin-compatible thermodynamic data base. The calculations using this mechanism in this report use this thermodynamic data base. We have done calculations using the Schmitt/Alkam

mechanism[2,3] using the GRI thermodynamic data base with the addition of properties for CH_3O_2, and several other less important alkyl peroxides, calculated using THERM[4]. These species are included in the Schmitt/Alkam mechanism, but not in the GRI or Chemkin data base. All calculations are done using the SENKIN driver package[5] at constant pressure and temperature conditions.

The calculations were done at a system pressure of 250 bar over a temperature range of 420 - 630 °C and assume the ideal gas equation of state for all species, including water. As a result, the number density of water is always lower in the calculation than it would be using an exact equation of state for water. However, changes in the water concentration on the order of 10-20% affect the overall quantitative results very little. It is likely that the error in the water density will become more important below 420 °C at this pressure.

Oxygen is used as the oxidizer at an equivalence ratio of 0.75 for most of the calculations. When oxygen concentration is varied in the results presented below, the equivalence ratio is listed. In the examples where fuel concentration is varied, the oxygen is varied accordingly to preserve an equivalence ratio of 0.75. Moderately lean conditions such as these are likely to be used in industrial SCWO systems.

Some of the comparison with experiment is done by way of an effective first order rate constant, k_{eff}, defined for the purposes here to be the reciprocal of the time at which the initial fuel mole fraction has fallen to 1/e of its original amount. This permits us to combine the results of experiments and calculations at different temperatures and feed concentrations on a single graph. Unfortunately, other observations from this analysis simultaneously illustrate that these reactions generally are not first order when the fuel concentration is varied over a wide range. In addition, distinct induction times are typical for these and similar reacting systems.[6-8] Despite these problems, use of k_{eff} is still the simplest way to represent the reaction rate when comparisons are done for a range of conditions where the reaction rate varies over several orders of magnitude.

Methane

Figure 1 shows the results from several calculations for the oxidation of methane at 420 °C, 450 °C, 550 °C, and 630 °C. Included on the figure are experimental data from earlier work[9,10]. The references contain the details of the experimental methods and data analysis. The solid line for the results at 0.1 mole/l from T= 390 °C to 440 °C are from a global fit to dozens of experiments at 270 bar at this initial fuel concentration. The reactions in these experiments were followed continuously to approximately 0.01 mole/l. The global fit produces the relationship

$$- d[CH_4]/dt = 10^{17.1} \exp(-30100/T) [CH_4]^{1.84} [O_2]^{-0.06} \quad (1)$$

where the concentrations are in mole/l and the pre-exponential-factor units are chosen so the rate is in mole/l-s. The dashed line marked as 0.003 mole/l is from a

calculation of $d[CH_4]/dt$ using Equation 1, extrapolated to this lower concentration. This calculated $d[CH_4]/dt$ can then be reexpressed as k_{eff} by writing

$$- d[CH_4]/dt = k_{eff} [CH_4] . \quad (2)$$

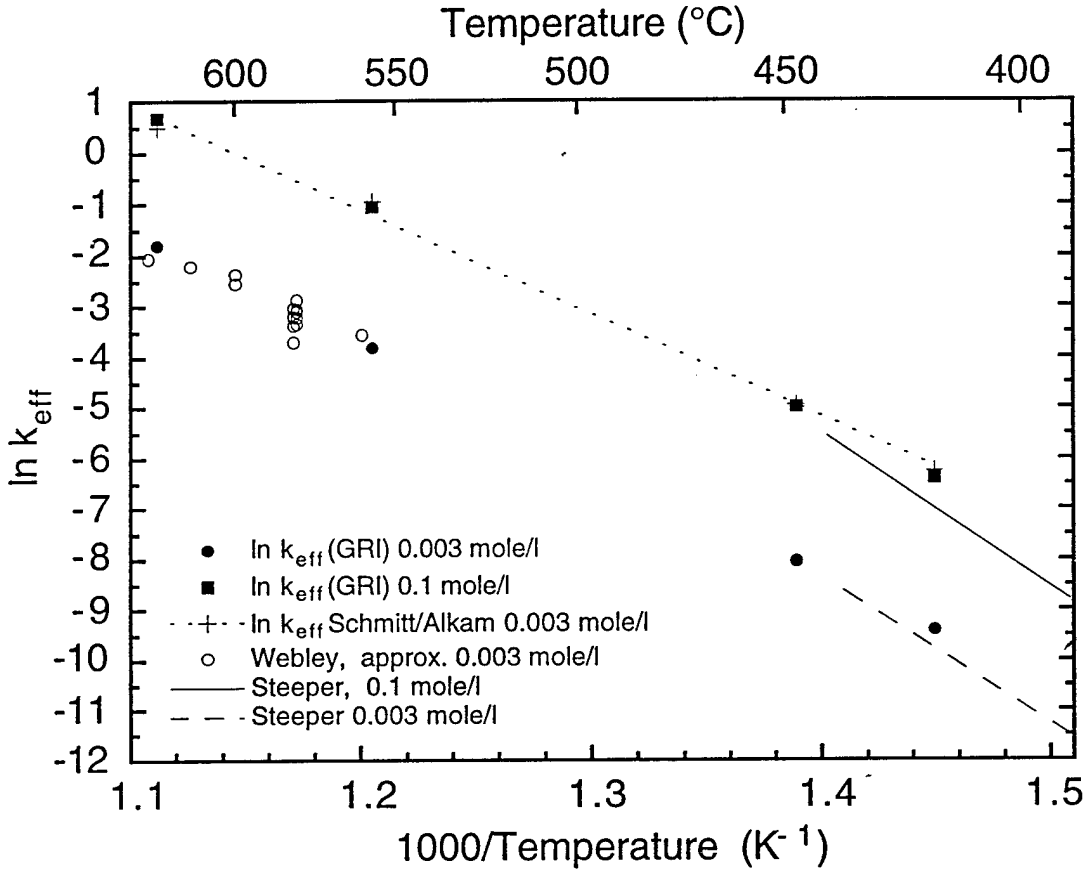

Figure 1. Comparison of calculated effective first order rate constants, k_{eff}, for the oxidation of methane from the GRI 1.2 mechanism and experimental results from Ref. 9 and 10. Also included are the predictions from Ref. 2 at low concentration.

Because the global fit produces an exponent of 1.84 for the fuel concentration, the first order k_{eff} calculated at 0.003 mole/l is less than at 0.1 mole/liter. The experiments covered both lean and rich conditions, but no significant oxygen concentration dependence is observed. In addition, no significant induction period is observed in the experiment. The experiments reported in Ref. 9 were also conducted at both lean and rich conditions. A global fit to these data gives an expression for the fuel consumption as

$$- d[CH_4]/dt = 10^{11.1} \exp(-21500/T) [CH_4]^{0.99} [O_2]^{0.66} . \quad (3)$$

The agreement of the Chemkin calculation using the unmodified GRI mechanism with the experimental data is excellent. The calculation reveals fuel consumption curves that exhibit a brief induction period, which in general is a small fraction of the 1/e time constant. This shows that the GRI 1.2 mechanism accurately reproduces the fuel consumption rates for the oxidation of methane over the entire temperature range likely to be used in SCWO applications. The mechanism reproduces the absolute fuel consumption rate and shows a distinct reaction rate dependence on initial fuel concentration. The experiments show that the low temperature results extrapolate smoothly to data measured at high temperature.

Included on this plot is a similar analysis from the Schmitt/Alkam[2,3] reaction mechanism. This mechanism systematically predicts rates that are about an order of magnitude faster than is observed. The model presented by Brock and Savage[11], before adjusting parameters to reproduce the experimental data, is more accurate, but still overestimates the reaction rate for methane in the 550°C - 630°C region by about a factor of two. This corresponds to an error in the reaction temperature of 60 °C.

Figure 2 shows our proposed pathway of methane to CO_2 for the temperature and pressure range of our SCWO experiments (400 °C < T < 650 °C, 22 < P < 30 MPa). Only a very small fraction of the CH_3O is converted to methanol by reaction with water, so this path does not appear in the figure. In addition, because methanol is significantly more reactive than methane, it is not accumulated. In fact, no significant amount of transient non-radical species are accumulated, other than CO and CO_2. This is in contrast to the results for methanol oxidation where formaldehyde and hydrogen peroxide are produced in significant quantities.

Figure 3 shows a more complicated flux diagram for the oxidation of methane using the Schmitt/Alkam mechanism. The fundamental difference from the GRI mechanism is the presence of the rapid equilibrium reaction

$$CH_3+O_2+M <=> CH_3O_2+M \qquad (4)$$

The presence of this reaction directs the subsequent oxidation chemistry through CH_3O_2 until formaldehyde is reached. The route by which methane is oxidized is very different if this key reaction, and the subsequent reactions of CH_3O_2 as both an oxidizer and a fuel are included. These reactions are not included in the GRI mechanism.

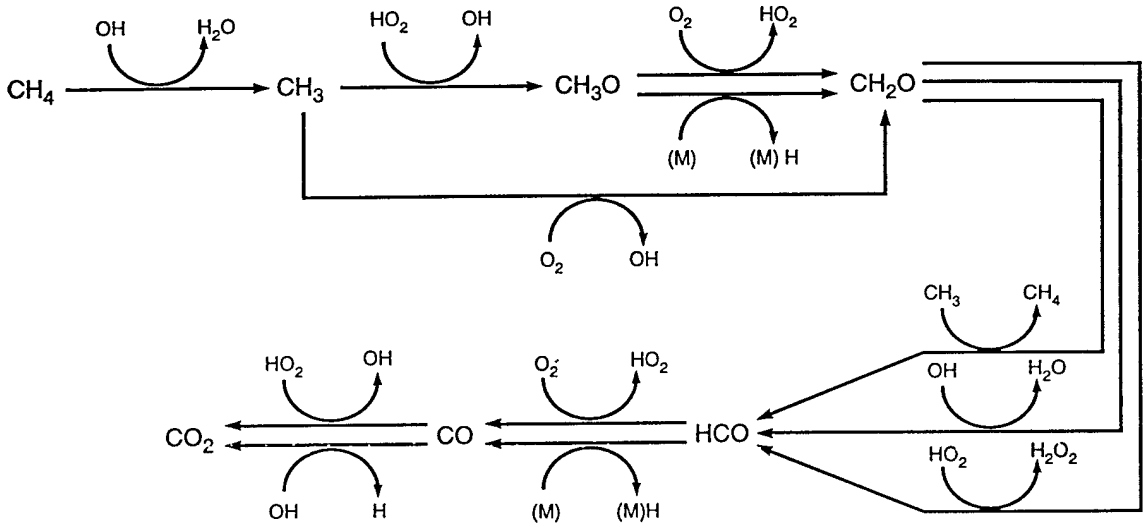

Figure 2. Flux diagram of the formation and consumption pathways of the major carbon species in the oxidation of CH_4 in supercritical water predicted by the GRI 1.2 mechanism.

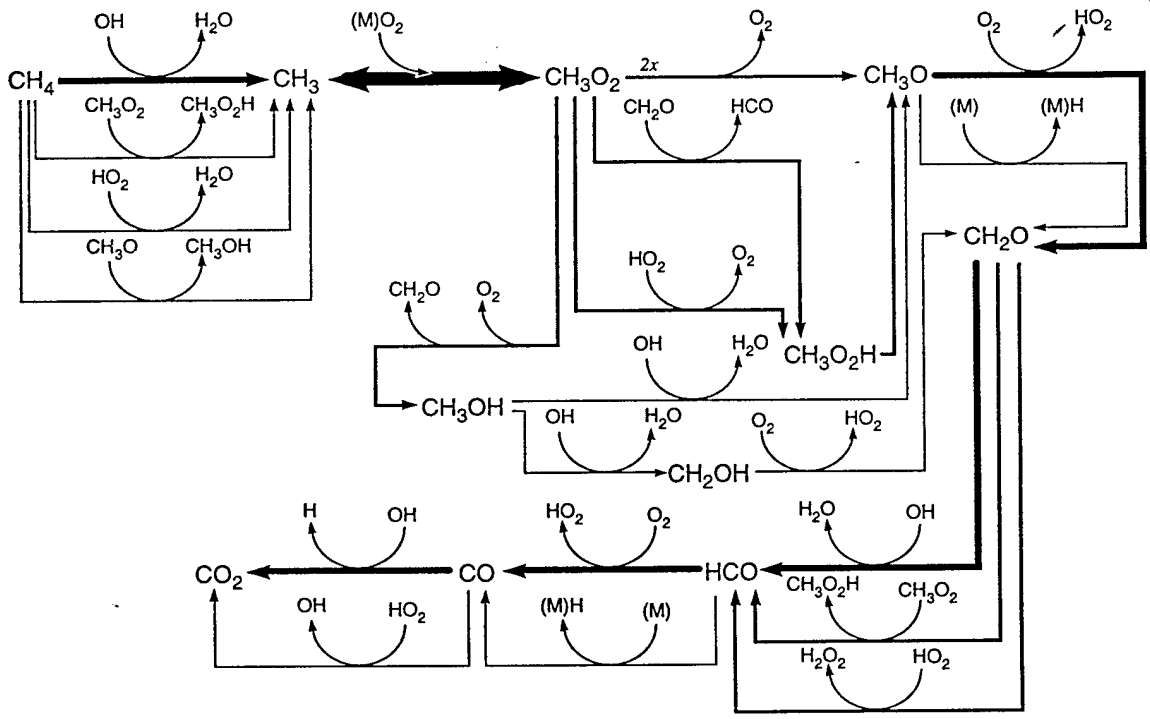

Figure 3. Flux diagram of the formation and consumption pathways of the major carbon species in the oxidation of CH_4 in supercritical water predicted by the mechanism described in Alkam et. al.[3].

The performance of the GRI mechanism can be evaluated on aspects other than the fuel consumption rates. The global fit in Equation 3 suggests that there is an oxygen concentration dependence of order 0.66. Table 1 shows GRI mechanism predictions for varying equivalence ratios at a constant fuel mole fraction of 0.0005 at 600 °C. The GRI mechanism shows a clear trend in acceptable agreement with Ref. 9. The calculated results fit very accurately to an oxygen concentration exponent of 0.734. However, the GRI mechanism also shows the same O_2 dependence at lower temperature in contrast to the global fit from Ref. 10, where no oxygen concentration dependence is seen. The same calculation using the Schmitt/Alkam model shows essentially no dependence on oxygen concentration. This suggests that the GRI mechanism does not fully represent the additional pathways associated with temperatures below 450°C.

Table 1

Effect of Oxygen Concentration on Rate of Methane Oxidation [a]

O_2 mole fraction	Equivalence ratio	k_{eff} (s^{-1})[b]	Fitted k_{eff} (s^{-1})[c]
0.0133	0.075	0.256	0.294
0.00665	0.15	0.182	0.176
0.00400	0.25	0.132	0.121
0.00266	0.375	0.102	0.090
0.00133	0.75	0.0571	0.0542
0.00100	1.0	0.0438	0.0439
0.00067	1.5	0.0284	0.0327

a - Initial methane mole fraction =5.0 x10^{-4}, T=600 °C, P=250 bar

b - Defined as $k_{eff} = 1/\tau$, with reaction time, τ, at $[CH_4]/[CH_4]_o = 1/e$.

c - Prediction from fit to k_{eff} = a (O_2 mole fraction)^b , with a= 7.018 and b=0.734

The inclusion of the rapid equilibrium with O_2 in the Schmitt/Alkam model serves to remove any oxygen dependence from the mechanism. It is possible that the GRI mechanism is appropriate at higher temperature, but the methylperoxyl chemistry must be included at lower temperature. The inaccurately high rates calculated at low O_2 concentration by the Schmitt/Alkam model in Figure 1 may originate from poor kinetic parameters and thermodynamics for the methylperoxyl chemistry. The issue requires further investigation.

Methanol

We recently reported significant new information on the oxidation of methanol and the simultaneous production of formaldehyde.[6] Last quarter, we began to compare the oxidation of methanol with the results from the GRI mechanism and showed that with the addition of two reactions,

$$CH_3OH + HO_2 => CH_2OH + H_2O_2 \quad (5)$$

and

$$CH_3OH + O_2 => CH_2OH + HO_2 \quad (6)$$

the fuel consumption profiles were fairly well reproduced by the model. The difference of rate at 500 °C was about a factor of two, but in this temperature range, this corresponds to an error in reaction temperature of only about 10 °C.

The GRI mechanism, supplemented with Reactions 5 and 6, still does not predict the accumulation of formaldehyde that we observe in this system; peak concentrations are calculated to be about a factor of five below the experimentally observed values. This is because the parameters chosen for the reaction

$$CH_2O + HO_2 => CHO + H_2O_2 \quad (7)$$

are not consistent with the values reported in Baulch et. al.[12] In the GRI mechanism, the Arrhenius parameters used produce a rate constant for the removal of formaldehyde that is too large. Figure 4 shows the results for the formation of formaldehyde as a fraction of the total amount of feed carbon, as methanol, compared to the prediction using the modified GRI mechanism when the parameters for Reaction 7 are changed to those reported by Baulch.[12] Significantly better agreement is achieved.

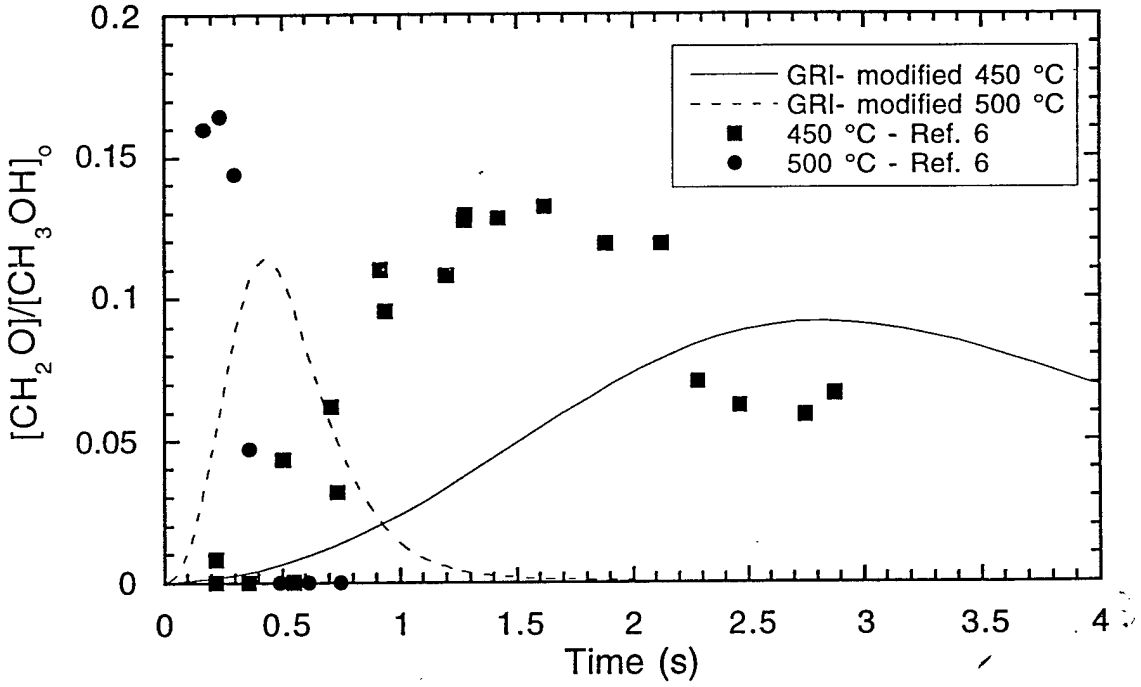

Figure 4. Comparison of experimental results from Rice et. al. [6] for the production of formaldehyde during methanol oxidation at 450 °C and 500 °C at 250 bar with the predictions from the GRI 1.2 mechanism with the modifications to HO_2+CH_3OH and HO_2+CH_2O. The expression $[CH_2O]/[CH_3OH]_o$ refers to the concentration of formaldehyde observed normalized by the initial methanol feed concentration.

Figure 5 shows the results of the GRI mechanism for the oxidation of methanol over a range of feed concentrations. The data marked "Raman" are determined using k_{eff} (the 1/e effective time constant) described in this report, based on the experiments in Ref. 6. The other data are from experiments using gas chromatography analysis from samples with reaction times of approximately 7 seconds.[6] The mechanism represents fairly well the change in effective rate constant for feeds of low and high fuel concentration. It also shows the apparent decrease in this effect as temperature is raised, although the agreement on this point is only qualitative.

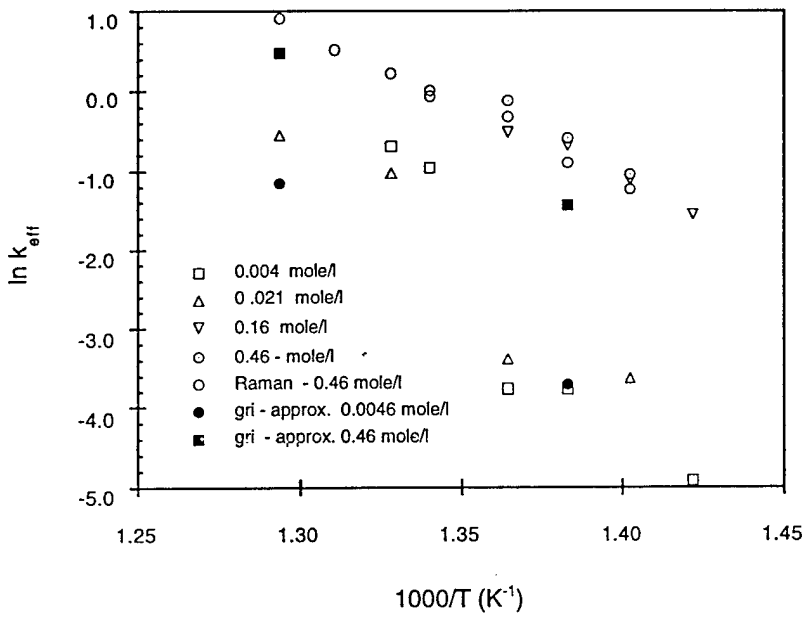

Figure 5 Comparison of the concentration dependence of methanol oxidation with experiments.[6] Because the temperature varies in this data set, concentration at reaction conditions is not constant. The concentrations reported are ambient temperature feed concentrations for both the experimental and the calculated values, for consistency. The actual concentrations at temperature and 250 bar are approximately a factor of 10 less, and may be calculated by using an equation of state for water. For example, at 500 °C and 250 bar the density of water is 0.0899 g/cm^3, yielding reaction concentrations about a factor of 11 lower than the feed concentrations. The mole fractions remain constant.

Conclusions

The recently developed GRI 1.2 methane oxidation mechanism has been applied to the oxidation of methane and methanol by oxygen in water at 250 bar and temperatures ranging from 420 - 630 °C. These conditions deviate substantially from the much higher temperature and lower pressure conditions for which it was designed and optimized. The results for the oxidation of methane with no modification of the mechanism agree very well with the available experimental results at these conditions. However, there is some evidence that the mechanism may be incomplete when applied to the <450 °C range, perhaps because the GRI mechanism does not contain CH_3O_2 chemistry. Mechanisms that contain this chemistry may be required to properly represent oxygen dependence of the lowest temperature methane oxidation data. To represent properly the oxidation of methanol and the formation of formaldehyde, three modifications to the GRI 1.2 mechanism were required. With these simple modifications, good agreement is achieved, for the temperature range of 440°C to 500 °C and pressures near 25.0 MPa.

Isopropanol and n-propanol oxidation

The results on isopropanol that we have reported recently[7] were interesting in that a well-defined stable intermediate, acetone, was produced in significant quantity resulting in a delay in the release of heat from the oxidation of this species. Because of the interest in using isopropanol or other alcohols as a supplemental fuel in certain reactor configurations, the rate of the complete oxidation process to CO_2 has significant reactor design implications. From a mechanistic perspective, in extending our C_1 model to higher alcohols, we will need to determine if isomeric differences such as in n-propanol vs. isopropanol are important.

We have undertaken a series of experiments in the SFR to compare directly the oxidation of isopropanol and n-propanol. Using Raman spectroscopy as the analytical tool, we have been able to follow the loss of fuel, production of intermediates including CO, and finally the production of CO_2 during the oxidation of isopropanol and n-propanol under SCWO conditions.

Figure 7a shows the loss of isopropanol as a function of temperature and time and Figure 7b shows the corresponding data for n-propanol. The figures show that the loss of n-propanol is slightly faster at a given temperature than the loss of isopropanol, such that comparable reactivity for n-propanol occurs about 20 °C lower than for isopropanol. This is only part of the picture, however.

Figure 8a and 8b show the fraction of the carbon in the system that exists as CO as a function of time and temperature during the oxidation of isopropanol and n-propanol and Figure 9a and 9b show corresponding fractions of CO_2. In the case of n-propanol, much more of the initial reactant is converted to CO and CO_2 early in the reaction than is the case for isopropanol. For example, in the case of n-propanol at 430 °C and 1.0 seconds, 20% of the carbon exists as CO_2, 40% exists as CO_2, and the remaining 40% as n-propanol. At 2 seconds these values are 35%, 55%, and 10% respectively. For isopropanol these values are 0% CO_2 and CO and 80% isopropanol at 1 second and 10 % CO_2 ,15% CO, and 30% isopropanol, at 2 seconds. Much of the carbon during the oxidation of isopropanol exists as some other species, whereas in the case of n-propanol the route to CO and CO_2 is faster, with no apparent carbon-containing intermediate being accumulated.

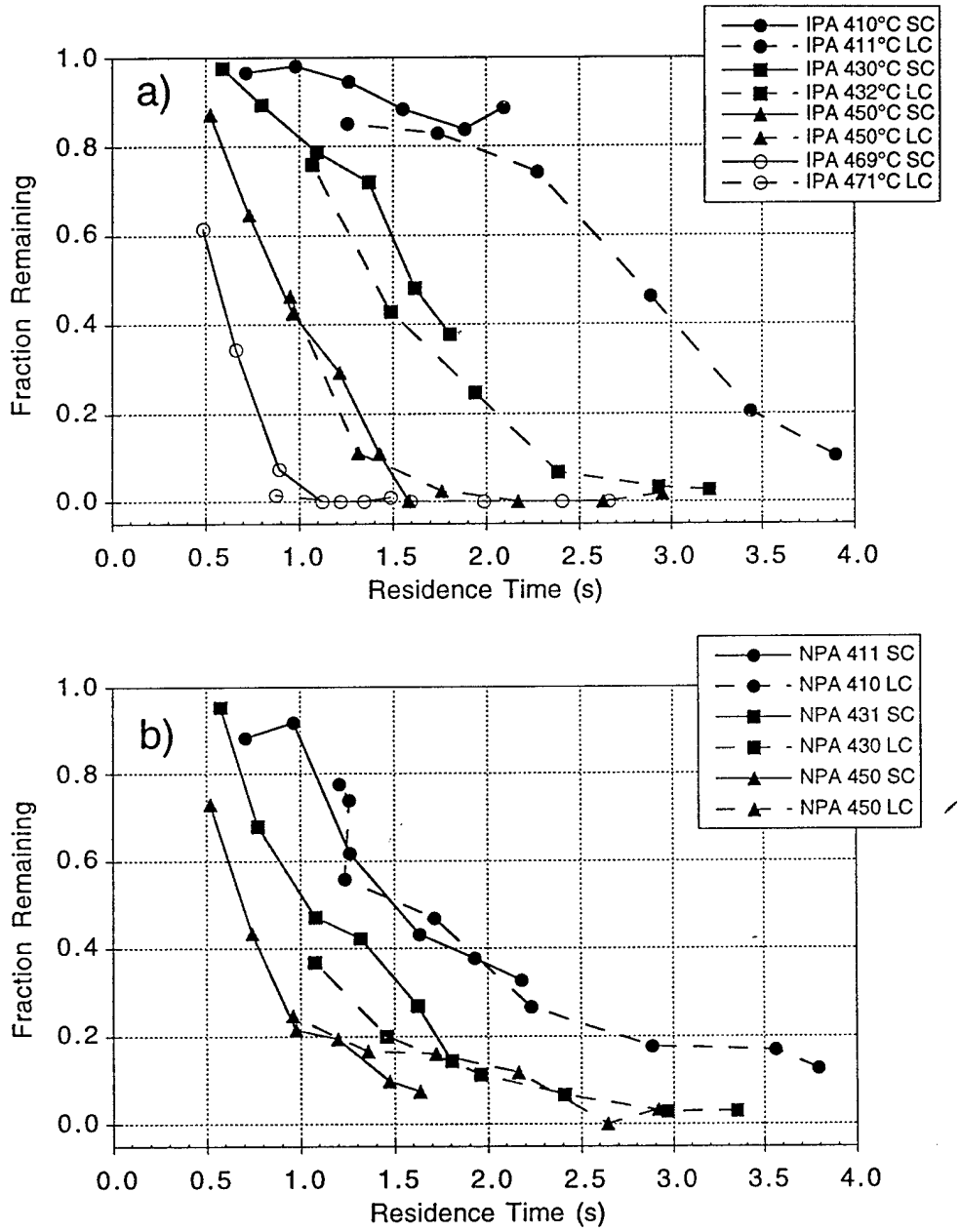

Figure 7. a) Oxidation of isopropanol by oxygen in supercritical water at four different temperatures at 25.0 MPa. The label on the ordinate, Fraction Remaining, refers to the fraction of feed isopropanol remaining at each measurement point (time) as detected by Raman spectroscopy. The "long and "short" positions of the cell in the flow reactor are 44.5 cm (SC) and 81.3 cm (LC). The different residence times for fixed cell positions are obtained by varying the total flow rate. b) Oxidation of n-propanol by oxygen in supercritical water at three different temperatures at 25.0 MPa. The experimental methods were the same as used for isopropanol described above.

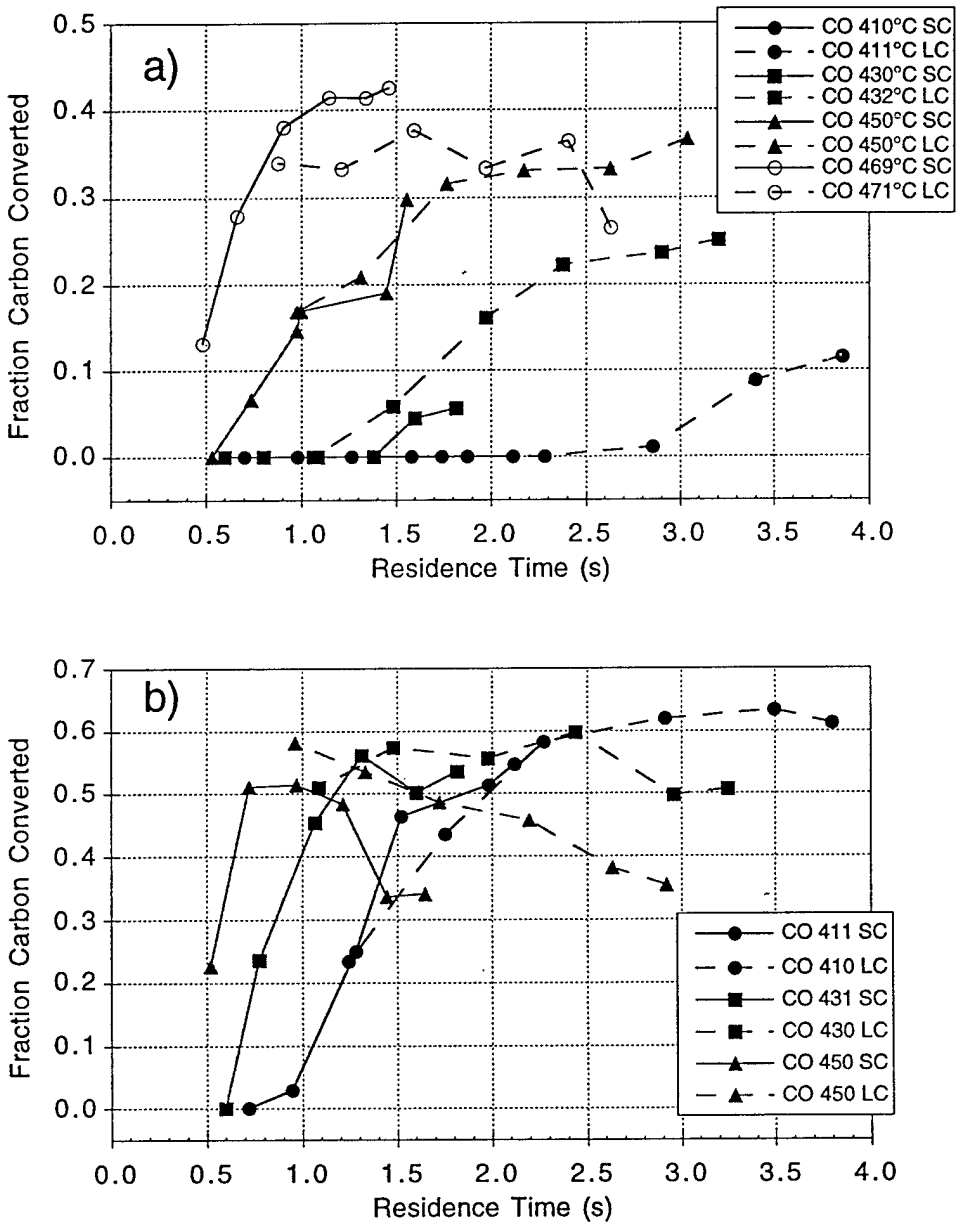

Figure 8. a) Production of CO during the oxidation of isopropanol in supercritical water at four different temperatures by oxygen at 25.0 MPa. Fraction Carbon converted refers to the molar fraction of initial feed alcohol that exists as CO. b) Production of CO during the oxidation of n-propanol in supercritical water at three different temperatures by oxygen at 25.0 MPa. The experimental methods were the same as for isopropanol described above.

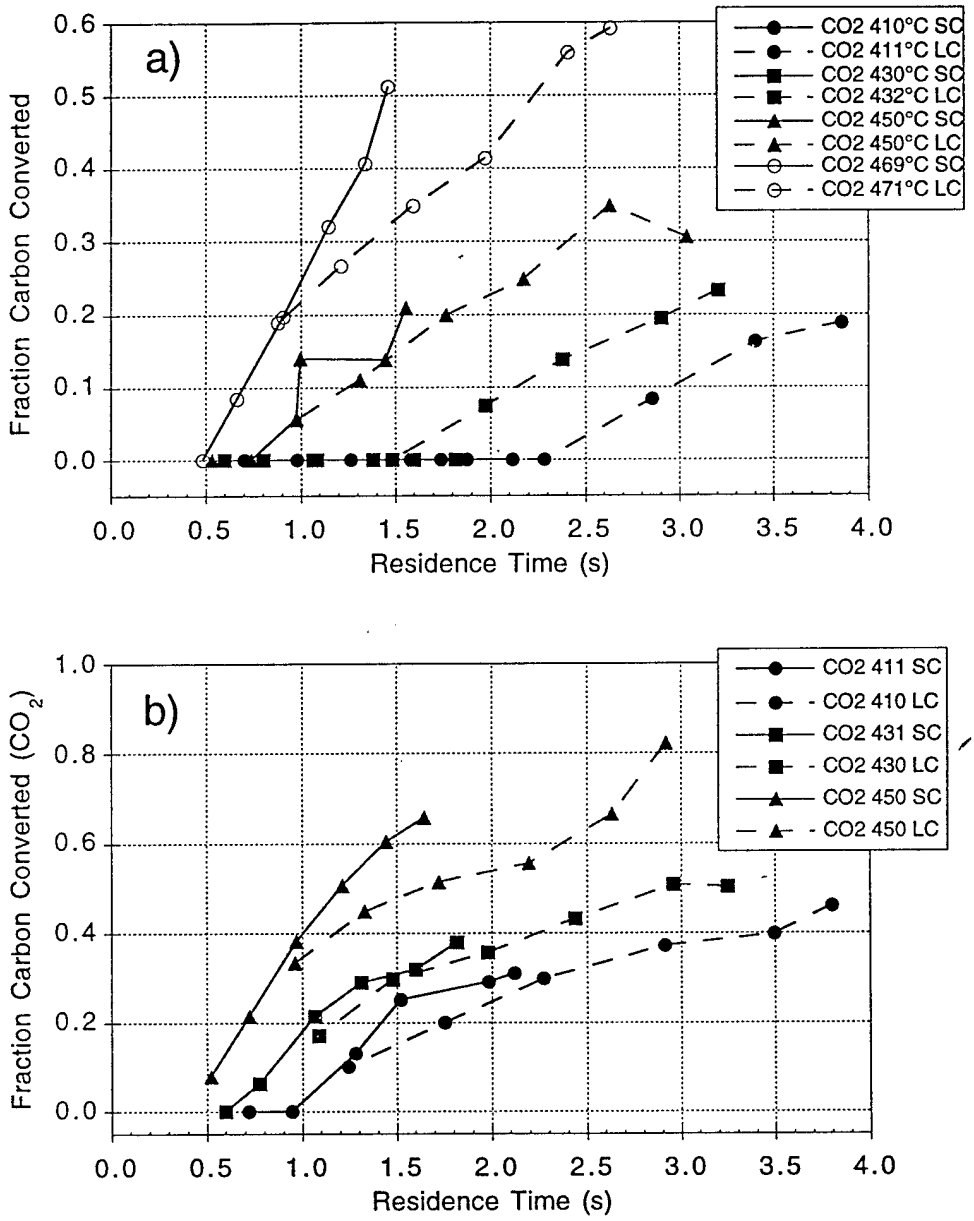

Figure 9. a) Production of CO_2 during the oxidation of isopropanol in supercritical water at four different temperatures by oxygen at 25.0 MPa. Fraction Carbon converted refers to the molar fraction of initial feed alcohol that exists as CO_2. These data were recorded sequentially with the results in Figure 7 and 8. b) Production of CO_2 during the oxidation of n-propanol in supercritical water at three different temperatures by oxygen at 25.0 MPa. The experimental methods were the same as for isopropanol described above.

Figure 10 shows the fraction of carbon existing as acetone in the oxidation of isopropanol at 430 °C is 20% at 1 s and 40 % at 2 seconds. The data show that in the case of isopropanol the formation of a stable ketone, acetone, will significantly slow the rate of conversion of organic to CO and CO_2. The same trends are true over the entire temperature range that has been examined.

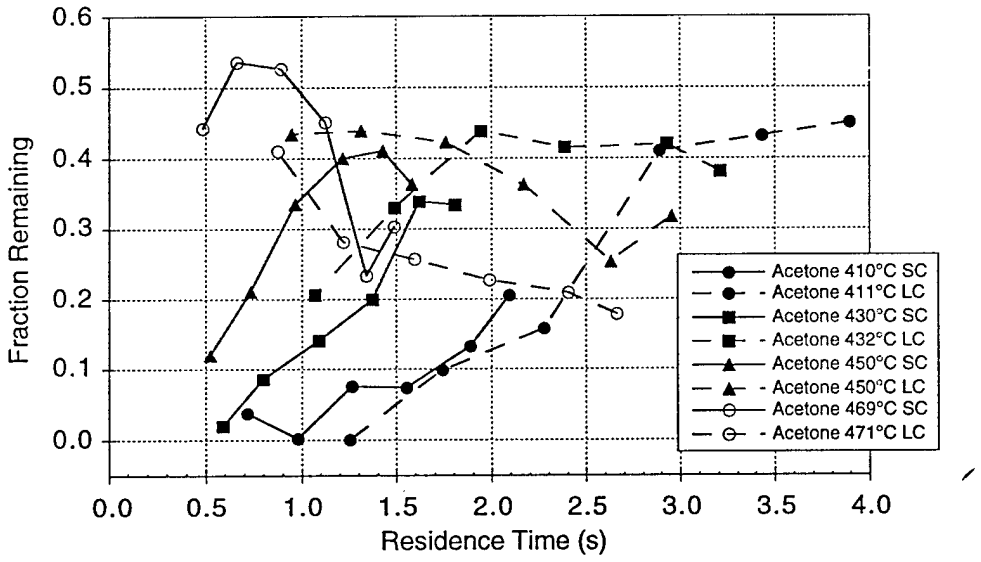

Figure 10. Production of acetone during the oxidation of isopropanol in supercritical water at four different temperatures by oxygen at 25.0 MPa. Fraction remaining refers to the molar fraction of initial feed isopropanol that exists as acetone. These data were recorded sequentially with the results in Figure 7a, 8a, and 9a.

Water gas shift reaction

Nine more experiments were conducted examining the water gas shift reaction in supercritical water at 450 °C over a pressure range of 2.0 - 29.0 MPa (~300 - 4300 psia). The results are interesting and indicate the further refinements in our experimental approach are needed.

It appears that at least one and maybe several different "side products" are formed during this reaction in addition to the main process forming CO_2 and H_2. These "side product" species have Raman features at 1040, 817, 588, and 412 cm^{-1}. We are in the process of establishing how many of these lines are proportional to each

other, which would suggest, but not assure, that they are Raman resonances for the same molecule.

To date our attempts to identify these side products have been unsuccessful. We had hoped to be able to show that some of these features were due to formic acid, since it is postulated to be an intermediate in this overall mechanism. However, none of the observed Raman features correspond to lines in the Raman spectrum of formic acid. In fact no features are seen in a scan in the 2700 - 3000 cm^{-1} region, indicating that, not only is no formic acid present, but also there are no species present that have a C-H bond, such as formic acid, formaldehyde, or many other possible organic species.

The best candidate appeared to be carbon suboxide C_3O_2, an unusual, but stable molecule known to have Raman lines at 584 and 820 cm^{-1}.[13] It also has a strong resonance at 2185 cm^{-1}. Unfortunately, our data show no lines near 2185 cm^{-1} other than the nearby CO resonance. Thus C_3O_2 can be ruled out.

Kruse and Franck [14] have observed the presence of a feature at 1017 cm^{-1} in water containing carbon dioxide at 75.0 MPa and have also observed a feature at 1060 cm^{-1} in water at 300 °C and high pressure. In these experiments, they observe a shift in the feature that moves to lower energy as temperature is raised. It is possible that this feature at 1060 cm^{-1} is the same one that they see at 1017 cm^{-1} under different pressure and temperature conditions. They suggest that it is due to carbonic acid, H_2CO_3, the hydrated form of CO_2. This would imply that that the overall process in our reactor is not simply the water gas shift. Rather, according to their suggestion, the overall reaction of $CO+H_2O$ =>[H_2CO_2 (formic acid)] => CO_2+H_2 is complicated by CO_2+H_2O => H_2CO_3, disturbing the equilibrium of CO/CO_2.

Although the experiment is clearly more complicated that the simple system we had hoped to be using as a way of isolating water's participation in changing transition state energies, we are confident that these complications can be sorted out in the future to permit the analysis of the $CO+H_2O$ data as intended.

Massachusetts Institute of Technology

This work was supported partly by the SERDP program through contract LD-1653 at Sandia National Laboratories and partly by the Army Research Office University Research Initiative Program. Prof. Jefferson W. Tester is the lead researcher on this sub-project for SERDP. This work is designed to compliment and in some cases provide an independent check on the experiments that are conducted at Sandia. In addition, a significant aspect of this work is to contribute to the development of a C.H,O general oxidation model, a major goal of this SERDP project.

Hydrogen peroxide/oxygen feed

We are investigating the use of hydrogen peroxide as an alternative source of oxygen (O_2) in our bench-scale, oxidant feed systems. Due to the low solubility of oxygen in water, current saturator-based feed arrangements are limited to inlet concentrations of less than about 0.4 wt% oxygen. Inlet organic concentrations are similarly limited by their poor solubility in water. The intent of the new oxidant feed system is to address this limitation and extend the range of operability of our bench-scale systems to higher organic and oxygen feed concentrations. This new oxidant fuel system eliminates the need for gaseous oxygen compression and allows us to examine higher molecular-weight organic wastes, while maintaining sufficient air-fuel ratios for complete combustion.

In the new delivery system, an aqueous hydrogen peroxide feed solution is fed under pressure to a Hastelloy vessel maintained at supercritical temperature (~ 400-450 °C). While in the reactor at these conditions, the hydrogen peroxide in solution is allowed sufficient residence time to undergo complete decomposition to oxygen and water via the following reaction: $H_2O_2 = 1/2\ O_2 + H_2O$. Experimental data from published hydrogen peroxide decomposition work indicates that a residence time of 60 seconds at 300°C should result in 99.9% decomposition of the peroxide. The resulting oxidant stream, now containing dissolved oxygen instead of peroxide, is then preheated to SCWO reaction conditions and fed as a homogeneous supercritical phase to the mixing tee of the primary reactor. Preliminary control experiments with this system indicate that hydrogen peroxide is decomposed effectively in our system and the resulting amount of oxygen produced is in agreement with the following overall stoichiometry of the peroxide decomposition reaction.

Since any hydrogen peroxide remaining undissociated after the holdup region will serve as a ready source of highly-reactive OH radicals, our principal concern with the design is the extent and rate of H_2O_2 decomposition that can be attained in the subcritical reactor. In order to determine whether the observed oxidation rate is the same with both the saturator-based and hydrogen peroxide O_2 feed systems (which it should be if the H_2O_2 decomposition reaction goes to completion), we are currently conducting methanol oxidation studies with both systems.

Feed mixing effects

We have redesigned the mixing tee at the entrance to our bench-scale tubular reactor in an effort to improve the degree of mixing in the reactor entrance region. The redesign was carried out largely due to the short timescales over which SCWO reactions occur (0-20 seconds in our system at temperatures of 500-600°C) and our concern about possible segregation of oxidant and organic during the first few seconds of contact, which would adversely impact the observed kinetics. As a result of analysis and a review of recent literature research aimed at identifying optimal micromixing conditions in pipeline tees, we have increased the turbulence levels by constricting apertures and have adopted a side-entry inlet tee configuration (oxidant and organic feed streams entering the tee at a 90° angle to each other). Reynolds

number in both the main and side-branch streams of the new tee range from 11,000 to 15,000 under normal operating conditions.

Use of the new mixing-tee design in recent methanol oxidation experiments revealed that the observed induction time (initially thought to be entirely a kinetic phenomena) is much shorter than that seen in experiments using the old design. Methanol oxidation experiments with the new tee design show little to no apparent induction time, while those using the older tee show induction times of 1-2 seconds. Thus, it appears that previous experimental SCWO data obtained using the old tee are partially confounded by a mixing time effect. We are hopeful that a systematic correction can be applied to our data and efforts are currently underway to reexamine key compounds and determine the extent to which the conversion data or rate expressions based thereon are affected by the mixing time phenomenon.

Princeton University

This work was supported by the SERDP program through contract LD-1652 at Sandia National Laboratories. Dr. Kenneth Brezinsky is the lead researcher. This work is designed to develop a detailed model for the combustion chemistry of simple aromatics, phenol and anisole, at temperatures near combustion conditions in the presence of excess water. Unlike the case of methane and methanol, where good elementary schemes existed at combustion conditions, there are not reliable combustion mechanisms to begin to modify for SCWO conditions. The special considerations of having a large excess of water present will illuminate the potential role that hydrolysis chemistry may play by competing with oxidation.

Species mole-fraction-versus-time profiles for intermediates formed during the high temperature, atmospheric pressure, gas phase pyrolysis and oxidation of anisole were obtained. This data set, spanning a range of stoichiometries (from 0.59 to 1.62) at two temperatures (730 °C and 910 °C), will serve as the benchmark for investigation of the water-perturbed gas phase system and, ultimately, the supercritical water oxidation chemistry of anisole. The reliability of the experimental data is evidenced by uniform carbon totals and repeatability. Furthermore, the identities and relative quantities of observed reaction intermediates are consistent with the findings of other investigators.

These experimental measurements were conducted in a high-temperature, ambient-pressure flow reactor, specially configured to accommodate liquid and molten sample feeds. Analysis of the products is achieved by sample-and-quench methods followed by detailed gas chromatography and mass spectrometry. Details of the methods will be presented in the next report.

Experiments at 730 °C have revealed the stoichiometry independence of the initial fuel decomposition. Even in the presence of oxygen, the disappearance of anisole is dominated by its unimolecular decomposition to phenoxy and methyl radicals.

Phenol, cresols, ethane, and methane, recombination products of the methyl and/or phenoxy radicals, are major reaction intermediates and their yields are virtually independent of stoichiometry as well. Other stoichiometry-independent products include benzene, toluene, and cyclopentadiene. Yields of the two remaining major species, carbon monoxide and methylcyclopentadiene, do exhibit a distinct dependence upon stoichiometry suggesting a preferential oxidation of the latter. As expected for the oxidation experiments, some C_3-C_5 oxidation products were detected. However given the apparent insignificance of oxygen in this system, it is not surprising that these are merely trace species. Therefore this lower temperature data, which captures the growth (and in many cases the maximum concentration) of the major species described above, demonstrates the dominance of pyrolytic chemistry in the production of early reaction intermediates in the anisole-oxygen system. The complementary higher temperature (1180 K) experiments capture the destruction of these species in which oxygen, as expected, plays and important role.

A parallel modeling effort has been undertaken. An existing 130 reaction step mechanism, developed for the oxidation of benzene and toluene, has been extended to include new reactions relevant to the pyrolysis of anisole. The experimental data suggests the existence of a multichannel reaction scheme to form a number of the major species directly from recombination of the phenoxy and methyl radicals. However, much of this chemistry is unknown and must be estimated. QRRK analysis has been employed in order to estimate reaction rate constants and validate the proposed chemistry.

Preparation for the ensuing water addition experiments has been completed. This involved the design, construction, and testing of a water injection system. The injector consists of two concentric inconel tubes. A pressurized flow of nitrogen in the outer tube atomizes a stream of distilled water as it is injected into the inlet section of the reactor, where it is quickly vaporized in the hot flow of nitrogen and oxygen. The water injection point is sufficiently far upstream of the fuel injectors so as to ensure complete mixing of the water vapor prior to introduction of the fuel. Tests of the system have verified that complete vaporization of the liquid water is achieved.

The flow reactor's fuel injection system, originally designed for liquid and gaseous fuels, has been modified to allow for melting of a solid reactant and accurate metering of the hot liquid flow rate. A motor driven syringe pump, able to maintain precisely a given flow rate of liquid, had been fitted with heaters allowing phenol to be melted in its reservoir and held at an appropriate temperature throughout the course of an experiment. As mentioned above, phenol and the phenolic species cresol are the dominant early reaction intermediates in the pyrolysis and oxidation of anisole. In the current study, anisole is exploited as a means of examining the oxidation chemistry of phenol and related species. The difficulties associated with the handling and preparation of a toxic, room-temperature solid reactant like phenol have, in the past, hindered its use as a flow

reactor fuel. With the recent modification described above, however, direct oxidation studies of phenol may commence which will parallel those of anisole.

Plans for next quarter

Experiments will continue on the water gas shift task in the SCR, with special emphasis placed on achieving the highest possible density above the critical temperature to ascertain whether any dramatic effect can be seen due to high water concentration. We will also pursue the identification of the side products.

We will complete and submit the manuscripts for three papers on propanol oxidation, application of the GRI model to supercritical water conditions, and optical cell design. A Sandia report will be written describing the result of the ARPA/ONR Navy EHM oxidation rate measurements.. In addition, we expect to finally initiate the H_2O_2 photolysis experiments with Dept. 8351.

The SFR will be used for several different experiments next quarter. In addition to the SERDP flow reactor work on H_2O_2 decomposition, some activity will focus on the task assigned to the SFR for Sandia's contribution to a project with Foster Wheeler and Aerojet. The work is supported by ARPA and managed through the Office of Naval Research. We will be measuring time/temperature/conversion profiles for several important Navy excess hazardous materials (EHM). The materials to be examined are jet aircraft fuel JP-5, oxidation-stabilized engine lubricating oil, and hydraulic fluid. These three materials constitute 52% of the 30,000 lbs/month EHM generated by a typical nuclear aircraft carrier. The results from these tests will feed directly into critical design decisions to be made by FW and Aerojet to meet the stringent space and weight requirements the Navy has placed on a shipboard EHM destruction unit.

References

1 M. Frenklach, H. Wang, C.-L. Yu, M. Goldenberg, C. T. Bowman, R. K. Hanson, D. F. Davidson, E. J. Chang, G. P. Smith, D. M. Golden, W. C. Gardiner, and V. Lissianski, (Information on the GRI project and mechanisms can be obtained from the WWW page, http://www.gri.org, 1995).

2 R. G. Schmitt, P. B. Butler, N. E. Bergan, W. J. Pitz, and C. K. Westbrook, in *1991 Fall Meeting of the Western States Section/The Combustion Institute* (University of California at Los Angeles, CA, 1991), pp. 19.

3 M. K. Alkam, V. M. Pai, P. B. Butler, and W. J. Pitz, *submitted Combustion and Flame* (1995).

4 E. R. Ritter and J. W. Bozzelli, *International Journal of Chemical Kinetics* **23,** 767-778 (1991).

5 A. E. Lutz, R. J. Kee, and J. A. Miller, , 3.0 ed. (Combustion Chemistry Division, Sandia National Laboratories, Livermore, CA, 1986).

6 S. F. Rice, T. B. Hunter, Å. C. Rydén, and R. G. Hanush, *submitted Industrial and Engineering Chemistry Research* (1995).

7 T. B. Hunter, S. F. Rice, and R. G. Hanush, *submitted Industrial and Engineering Chemistry Research* (1995).

8 J. C. Meyer, P. A. Marrone, and J. W. Tester, *Journal of the American Institute of Chemical Engineers,* submitted, Reactors, Kinetics, and Catalysis (1994).

9 P. A. Webley and J. W. Tester, *Energy & Fuels* **5,** 411-419 (1991).

10 R. R. Steeper, S. F. Rice, I. M. Kennedy, and J. D. Aiken, *Journal of Physical Chemistry* **100,** 184-189 (1996).

11 E. E. Brock and P. E. Savage, *AIChE Journal* **41,** 1874-1888 (1995).

12 D. L. Baulch, C. J. Cobos, R. A. Cox, C. Esser, P. Frank, T. Just, J. A. Kerr, M. J. Pilling, J. Troe, R. W. Walker, and J. Warnatz, *Journal of Physical and Chemical Reference Data* **21,** 411-429 (1992).

13 W. H. Smith and J. J. Barrett, *The Journal of Chemical Physics* **51,** 1475-1479 (1968).

14 R. Kruse and E. U. Franck, *Berichte Bunsenges. Phys. Chem.* **86,** 1036-1038 (1982).

INITIAL DISTRIBUTION

Dr. E. Fenton Carey, Jr.
U.S. Department of Energy (ST-60)
1000 Independence Avenue, S.W.
Room GA 155
Washington, DC 20585

Dr. Robert Marianelli
U.S. Dept. Of Energy
19901 Germantown Rd.
Germantown, MD 20874

Carl Adema
SERDP Program Office
Program Manager for Compliance and
Global Environmental Change
901 North Stuart Street, Suite 303
Arlington, VA 22203

Jenny Dowden
Labat-Anderson Incorporated
8000 Westpark Dr.
Suite 400
McLean, VA 22102

John Harrison
SERDP Program Office
901 North Stuart Street, Suite 303
Arlington, VA 22203

Jim Hurley
US AF AL/EQS
139 Barnes Drive, Suite 2
Tyndall Air Force Base, FL 32403

Richard Kirts
Naval Civil Engineering Laboratory
560 Laboratory Dr.
Port Hueneme, CA 93043-4328

Crane Robinson
Arament Research
Development & Engineering Center
(ARDEC)
SMCAR-AES-P
Building 321
Picatinny Arsenal, NJ 07806-5000

Dr. Peter Schmidt
Office of Naval Research
Chemistry Division
800 North Quincy Street
Arlington, VA 22217-5660

Dr. Robert Shaw
Chemical & Biological Sciences Div.
U.S. Army Research Office
Research Triangle Park, NC 27709-2211

Prof. Martin A. Abraham
The University of Tulsa
Department of Chemical Engineering
600 South College Avenue
Tulsa, OK 74104-3189

Prof. Joan F. Brennecke
University of Notre Dame
Department of Chemical Engineering
Notre Dame, IN 46556

Dr. Kenneth Brezinsky
Dept. of Mechanical and Aerospace
Engineering
Princeton University
PO Box CN5263
Princeton, NJ 08544-5263

Prof. Klaus Ebert
Kernforschungszentrum Karlsruhe
Institut fur Heisse Chemie
Postfach 3640
D-76021 Karlsruhe
Germany

Prof. Earnest F. Gloyna
University of Texas at Austin
Environmental and Health
Engineering
Austin, TX 78712

Prof. Keith Johnston
University of Texas at Austin
Chemical Engineering Dept.
26th and Speedway
Austin, TX 78712-1062

Prof. Micheal T. Klein
Chairman
University of Delaware
Chemical Engineering Dept.
Colburn Labs Academic Street
Newark, DE 19716-2110

Prof. Phillip E. Savage
University of Michigan
Chemical Engineering Department
Herbert H. Dow Building
Ann Arbor, MI 48109-2136

Prof. Jefferson W. Tester
Massachusetts Institute of Technology
Energy Laboratory
Room E40-455
77 Massachusetts Avenue
Cambridge, MA 02139

K.S. Ahluwalia
Foster Wheeler Development
Corporation
Engineering Science & Technology
12 Peach Tree Hill Road
Livingston, NJ 07039

Dr. David A. Hazelbeck
General Atomics
M/S 15-100D
3550 General Atomics Court
San Diego, CA 92121-1194

Dr. Glenn T. Hong
MODAR, Inc.
14 Tech Circle
Natick, MA 01760

W. Killilea
MODAR, Inc.
14 Tech Circle
Natick, MA 01760

Richard C. Lyon
Eco Waste Technologies
2305 Donley Drive
Suite 108
Austin, TX 78758-4535

Dr. Michael Modell
Modell Environmental Corporation
300 5th Avenue, 4th Floor
Waltham, MA 02154

Phil Whiting
Abitibi-Price Inc.
2240 Speakman Drive
Mississauga, Ontario L5K 1A9
Canada

Marvin F. Young
Aerojet
PO Box 13222
Sacramento, CA 95813-6000

Dr. Graydon Anderson
LANL
P.O. Box 1663 MS-J567
Los Alamos, NM 87545

Dr. Steven J. Buelow
CST-6
Los Alamos National Lab.
Los Alamos, NM 87545

Philip C. Dell'Orco
Los Alamos National Laboratory
Explosives Technology & Safety C920
Los Alamos, NM 87545

Dr. Albert Lee
NIST
Bldg. 221 Room B312
Gaithersburg, MD 20899

Dr. William Pitz
LLNL
P.O. Box 808 L-014
Livermore, CA 94551-0808

Prof. Jean Robert Richard
CNRS
Combustion Laboratory
1C Avenue de la Recherche Scient.
Orleans 45071
France

Dr. Gregory J. Rosasco
Nat'l Institute of Standards and Technology
Division 836, Bldg. 221, Rm B-312
Gaithersburgh, MD 20899

Dr. Charles Westbrook
LLNL
P.O. Box 808 L-014
Livermore, CA 94551-0808

MS0828 P. J. Hommert, 1503

MS0701 R. W. Lynch, 6100

MS0735 D. E. Arvizu, 6200
6203 A. P. Sylwester
6211 G. A. Carlson
6212 H. R. Stephens

MS0756 G. C. Allen, 6607

MS9001 T. O. Hunter, 8000
Attn: 8100 M. E. John
8200 L. A. West
8400 R. C. Wayne
8800 L. A. Hiles

MS9214 C. Melius, 8117

MS9054 W. J. McLean, 8300

MS9042 C. Hartwig, 8345

MS9051 L. Rahn, 8351

MS9055 F. Tully, 8353

MS9056 G. Fisk, 8355

MS9052 D. R. Hardesty, 8361 (2)

MS9052 S. W. Allendorf, 8361

MS9052 M. D. Allendorf, 8361

MS9052 L. L. Baxter, 8361

MS9052 S. G. Buckley, 8361

MS9052 S. P. Huey, 8361

MS9052 M. M. Lunden, 8361

MS9052 T. A. McDaniel, 8361

MS9052 D. K. Ottesen, 8361

MS9052 C. Shaddix, 8361

MS9052 F. Teyssandier, 8361

MS9052 J. Aiken, 8361

MS9052 E. Croiset, 8361

MS9052 R. Hanush, 8361

MS9052 S. Rice, 8361 (20)

MS9053 R. Carling, 8362

MS9053 R. Steeper, 8362

MS9053 R. Gallagher, 8366

MS9101 B. Peila, 8411

MS9406 B. Haroldsen, 8412

MS9406 H. Hirano, 8412

MS9406 C. LaJeunesse, 8412

MS9406 M. C. Stoddard, 8412

MS9007 J. Swearengen, 8419

MS9404 B. Mills, 8713